THE JOURNAL OF PHYSICAL CHEMISTRY C

Article

pubs.acs.org/JPCC

The Role of Transport Agents in MoS_2 Single Crystals

Andrea Pisoni,*[,†] Jacim Jacimovic,[†] Osor S. Barišić,[§] Arnaud Walter,[†] Bálint Náfrádi,[†] Phillipe Bugnon,[‡] Arnaud Magrez,[‡] Helmuth Berger,[‡] Zsolt Revay,[∥] and László Forró[†]

[†]Laboratory of Physics of Complex Matter and [‡]Single Crystal Growth Facility, EPFL, CH-1015 Lausanne, Switzerland

[§]Institute of Physics, Bijenička c. 46, HR-10000 Zagreb, Croatia

[∥]Heinz Maier-Leibniz Zentrum (MLZ), Forschungsneutronenquelle Heinz Maier-Leibnitz (FRM II), Technische Universität München, D-85747 Garching, Germany

Supporting Information

ABSTRACT: We report resistivity, thermoelectric power, and thermal conductivity of MoS_2 single crystals prepared by the chemical vapor transport (CVT) method using I_2, Br_2, and $TeCl_4$ as transport agents. The material presents low-lying donor and acceptor levels, which dominate the in-plane charge transport. Intercalates into the van der Waals gap strongly influence the interplane resistivity. Thermoelectric power displays the characteristics of strong electron−phonon interaction. A detailed theoretical model of thermal conductivity reveals the presence of a high number of defects in the MoS_2 structure. We show that these defects are inherent to CVT growth method, coming mostly from the transport agent molecules inclusion as identified by total reflection X-ray fluorescence analysis (TXRF) and in-beam activation analysis (IBAA).

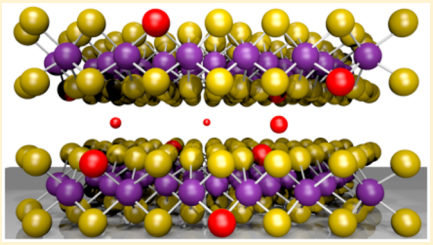

Molybdenum disulfide, MoS_2, has been known for a long time as a mineral, but the first detailed studies were performed in the 1970s, during the vivid interest for transition metal dichalcogenides.[1] This class of materials possesses a variety of electronic ground states, such as superconductivity, periodic lattice deformation (charge density waves), Mott transition, exciton formation, etc.[2−4] Within this cavalcade of fascinating properties, MoS_2 was left aside, since it had turned out to be a simple, indirect band gap (Δ) semiconductor[5] of Δ = 1.2 eV.

The revival of interest in this material has come with the isolation of graphene from graphite. Mechanical exfoliation of MoS_2 is also possible, and it still remains the preferred technique for obtaining single or few layers of this material.[6,7] MoS_2 single layers achieved by chemical or mechanical exfoliation have been extensively studied for both scientific and applicative purposes.[8−11] Chemical vapor transport (CVT) is the most used method to grow large area single crystals of transition metal dichalcogenides.[12,13] In order to obtain high quality MoS_2 few layers by exfoliation of single crystals, the good quality of the starting CVT-grown material must be ensured. Although other authors have already reported a dependence of the doping sign of WSe_2, $MoSe_2$, and WS_2 at room temperature on the transport agent used during the CVT growth,[12,13] a deeper and systematic study on how transport agents influence the electrical and thermal properties of MoS_2 single crystals is still missing. Moreover, a recent work has shown that chlorine doping can drastically reduce the width of the Schottky barrier between few layers of MoS_2 and metallic contacts allowing high performances in few layers MoS_2 field-effect transistors.[9] This observation demonstrates that inclusion of external atoms in MoS_2 can also be advantageous for applications.

We measured resistivity of single crystals grown by the CVT method using I_2, $TeCl_4$, and Br_2 as transport agents. Resistivity was measured parallel to the MoS_2 planes (ρ_{ab}) and out of planes (ρ_c). The possibility to measure ρ_{ab} down to 4 K is already strong evidence that charge transport is not dominated by the charge transfer gap. In fact, in the case of a pristine sample with Δ = 1.2 eV the resistivity would be so high that no measurable current would be able to pass through the sample even at room temperature. Both the in-plane and the out-of-plane ρ follow a $\rho_0 \exp(E_b/k_BT)$ temperature dependence (k_B is the Boltzmann constant, E_b is the impurity level activation energy, and ρ_0 is a temperature-independent constant). Figure 1 presents the Arrhenius plot of ρ_{ab} for a sample grown using I_2 as transport agent. The comparison between resistivities measured for different crystals obtained by the same CVT grown with iodine transport agent results in a scattering of ρ_0 and E_b values as shown in the inset of Figure 1. E_b is found in the 20−90 meV range. Because of the high level of doping, in some cases already at 100 K a conduction channel opens in the impurity band, and one observes very weak activation energy (4−5 meV). The low temperature flat part is presumably due to hopping conduction within the impurity band.[14]

Figure 2 shows a comparison between the measured ρ_c and ρ_{ab} for the same MoS_2 single crystal presented in Figure 1. The ratio ρ_c/ρ_{ab} = 100 at 300 K further increases on cooling. The extracted E_b = 0.3 eV for ρ_c is ∼6 times higher than for ρ_{ab}. In

Received: December 2, 2014
Revised: February 3, 2015
Published: February 5, 2015

DOI: 10.1021/jp512013n
J. Phys. Chem. C 2015, 119, 3918−3922

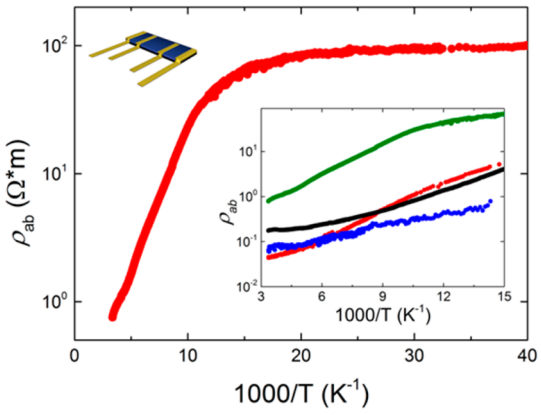

Figure 1. Arrhenius plot of the temperature dependence of the in-plane resistivity of a MoS_2 single crystal grown using I_2 as transport agent. The high temperature slope corresponds to a donor level at 50 meV below the conduction band. The different color lines in the inset correspond to resistivities measured for four different crystals obtained by the same CVT growth using the I_2 transport agent.

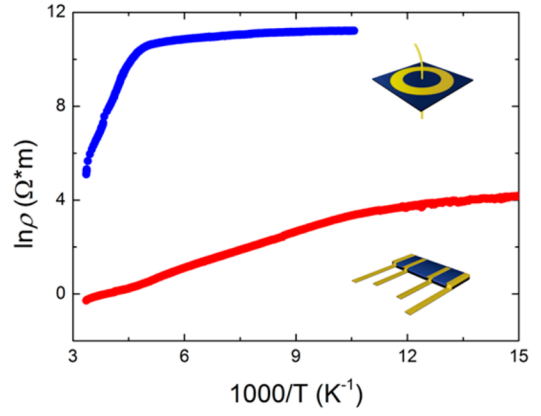

Figure 2. Arrhenius plot of the temperature dependence of the in-plane (red curve) and out-of-plane (blue curve) resistivities for a MoS_2 single crystal grown using I_2 as transport agent.

the high temperature regime, the temperature-dependent resistivity ratio suggests that the mechanism of conduction is different along the two directions. The higher activation energy for the interplane charge transport can be ascribed to intercalated atoms between the MoS_2 layers. In fact, ρ_c can be well described by $\rho_0 \exp(E_{int} + E_b/k_BT)$, where the additional energy barrier E_{int} is due to hopping process between nearest neighbors.[14] The charge carriers need phonon assisted hopping to get to the neighboring layer, and this phenomenon manifests itself as an additional activation term in resistivity.[14] Since the phonon assistance is diminishing with the lowering temperature, one observes a strongly increasing resistivity anisotropy.

Whether one deals with a donor or an acceptor impurity level may be deduced from the Seebeck coefficient (S). Figure 3 presents the Seebeck coefficient measured parallel to the MoS_2 planes for a sample prepared using I_2 as transport agent. The sign of S suggests that at high temperature the dominant type of charge carriers are hole-like (coming from an acceptor level), while at low temperatures the electron like charge carriers dominate (donor level). Furthermore, at room temperature S has a large value of 400 μV/K, typical for nondegenerated semiconductors.[15] In the latter case, S is given by

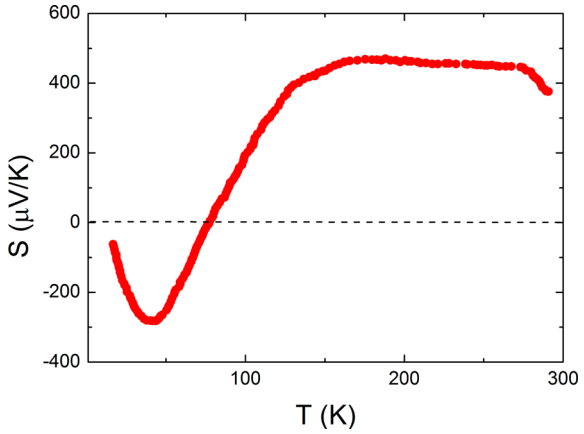

Figure 3. Temperature dependence of thermoelectric power measured along the MoS_2 planes for the sample grown by I_2 transport agent. Electron-like transport at low temperatures and hole-dominated one at high temperatures can be identified.

$$S = \frac{k_B}{e}\left(\frac{E_b}{k_BT} + \text{const}\right) \quad (1)$$

where e is the electronic charge. This expression gives an increase of $|S|$ with decreasing temperature. However, we find that S is temperature independent down to 180 K. Such behavior is characteristic of polaronic charge carriers,[16] which have been observed in other materials like boron carbide[17] and TiO_2 anatase.[18] In a simplified picture, the charge carrier excited to the conduction band polarizes the lattice and propagates along the lattice surrounded by this polarization. The energy involved in the creation of this new quasi-particle results with large values of S.

Thermal conductivity was measured for the MoS_2 sample prepared by I_2 transport agent. The results are presented in Figure 4. As for other poorly conducting materials, one may

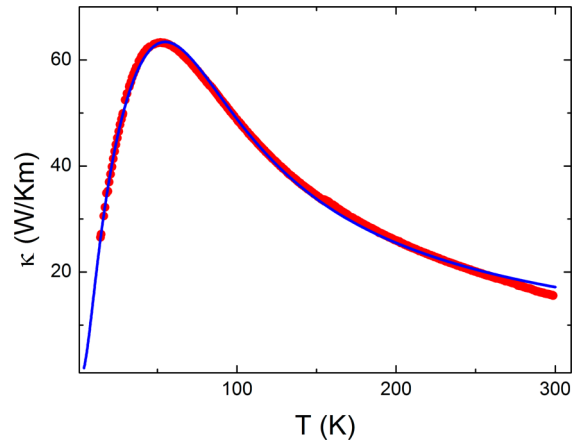

Figure 4. Temperature dependence of basal thermal conductivity of MoS_2 single crystal obtained using I_2 as transport agent. The blue curve represents the fit obtained by using eq 2.

expect that the dominant contribution to the thermal conductivity (κ) is of phononic origin. Indeed, assuming an electron density that justifies the usage of the Wiedemann–Franz law, one obtains a very low estimation for the value of the thermal conductivity due to charge carriers, being much less than 1 W/(K m). Therefore, one can safely neglect such term

DOI: 10.1021/jp512013n
J. Phys. Chem. C 2015, 119, 3918–3922

and analyze κ behavior in terms of purely phonon contribution. At room temperature we measured κ = 15 W/(K m), a value that is much lower than in other layered materials like graphite (κ = 2000 W/(K m)).[19] Room temperature thermal conductivity in a few and single layer MoS_2 was measured by a few authors. The measured data span between κ = 30 and 55 W/(K m), depending on the layer thickness and the way in which the samples were grown.[20−22] This is a clear indication that impurities and/or strong anharmonicities play a significant role. In particular, from 10 to 300 K, κ reveals three different temperature intervals: (i) the low temperature regime, below 40 K, where κ quickly diminishes as temperature decreases; (ii) the intermediate temperature regime, from 40 to 70 K, in which κ exhibits a maximum; and (iii) the high temperature part, from 70 to 300 K, in which κ becomes suppressed by temperature. This behavior has strong resemblances to other semiconducting materials and may be investigated in more details in terms of three independent mechanisms (relaxation times) for phonon scattering: Umklapp phonon scattering, impurity scattering, and sample boundary scattering.[23] With these three scattering contributions, in the context of the Callaway formalism, the integral expression for thermal conductivity due to the phonons is given by[23]

$$\kappa = CT^3 \int_0^{\theta_D/T} \frac{1}{a_1 + a_2 T^4 x^4 + a_3 T^3 x^2 \exp[-w_u/T]} \times \left[\frac{x^4 e^x}{(e^x - 1)^2}\right] dx \quad (2)$$

with $C = (k_B/2\pi^2 v_s)(k_B/\hbar)^3$, $x = \hbar\omega/k_B T$, θ_D is Debye temperature, k_B the Boltzmann constant, $\hbar$ the Planck constant, and v_s the average speed of sound. a_1, a_2, a_3, and w_u are parameters that should be determined from experiments, by using a fitting procedure.

All of the scattering mechanisms in eq 2 are active in the entire temperature range shown in Figure 4, however, not with equal importance. Phonon−phonon interaction is dominant at high temperatures, where, thanks to the thermal excitations, the phonon thermal occupation is high for almost all wavelengths and accompanied by strong anharmonicities. By lowering T, the phonon thermal occupation decreases and Umklapp scattering becomes less significant, which results in an overall rise of thermal conductivity. Yet, by further lowering the temperature, other scattering processes become more efficient. That is, effects of impurities start to dominate at about 1/5 of Debye temperature (θ_D = 500 K for MoS_2[24]). At very low temperatures, only the long-wave phonons remain in the system, with a mean free path being constrained by sample dimensions.

The values found for a_1, a_2, a_3, and w_u of eq 2 are given in Table 1. The corresponding fitting curve is shown in blue in Figure 4, nicely reproducing the experimental data in the entire temperature range. While the Umklapp scattering seems less efficient in comparison to results obtained for a semiconductor with similar values of Debye frequency and κ at room temperature (rutile TiO_2),[25] the scattering due to impurities is significantly enhanced for the MoS_2 sample. For the latter, a_2 is 2 orders of magnitude higher than for rutile TiO_2. This effect is additionally depicted by a low value of κ at the maximum with respect to the room temperature value, i.e., only a factor of 4, compared to a factor 100 observed in pure rutile TiO_2.[25] The expected low-temperature T^3 behavior is suppressed up to very low temperature, well below 15 K, which is the lowest temperature investigated in our experiment in Figure 4. All these findings show that our MoS_2 sample involves very strong scattering due to impurities. In particular, we believe that this effect should be ascribed to iodine contamination.

Table 1. Fitting Parameters by Using Callaway's Approach

a_1/C	a_2/C	a_3/C	w_u/C
1.8×10^6	0.69	2.09×10^2	200

The results presented so far indicate that the iodine transport agent causes an unintentional doping of the CVT grown MoS_2 and that the charge carriers have a polaronic character. The presence of transport agents into the bulk of MoS_2 single crystals was confirmed by IBAA and TRXF analysis (see Supporting Information). In the particular case of samples grown using I_2, TXRF reveals iodine contents up to 0.48 mol %. In order to investigate the effect of different transport agents on the electrical properties of MoS_2, we studied single crystals produced by $TeCl_4$ and Br_2 transport agents. Figure 5 shows

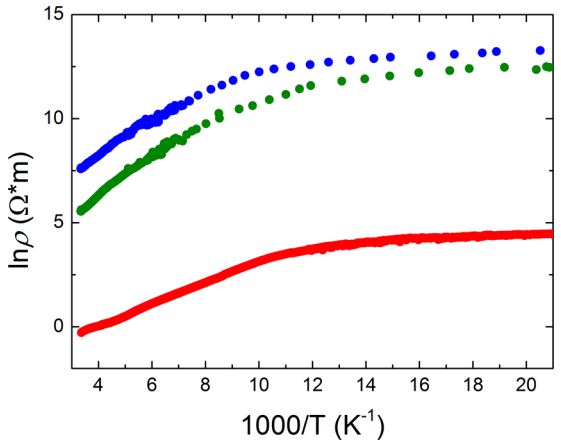

Figure 5. Arrhenius plot of the temperature dependence of the in-plane resistivity of MoS_2 single crystals grown by I_2 (red), $TeCl_4$ (green), and Br_2 (blue) as transport agents.

the comparison between Arrhenius plots of the in-plane resistivity of MoS_2 single crystals grown by the different transport agents. Similarly to the iodine case, we measured resistivity of different samples obtained by the same CVT growth using $TeCl_4$ and Br_2 as transport agents. The results (not shown here) present the same scattering in ρ_0 and E_b as displayed in the inset of Figure 1. In all the cases resistivity is measurable down to low temperatures and the temperature dependence is very similar; only the absolute value of ρ appears to be transport agent dependent. This could be due to different ways in which transport agents are incorporated into the crystal structure. In fact, the layered structure of MoS_2 offers interstitial sites,[26] and transport agents can intercalate between the MoS_2 layers. Iodine incorporation between planes of metal dichalcogenides has already been observed by scanning tunneling spectroscopy in other compounds grown by the CVT method in our laboratories.[27] Iodine can enter into the lattice by substituting S (forming $MoS_{2-x}I_x$) introducing one electron per formula unit. However, iodine can also be intercalated in between the MoS_2 layers. In this case the chemical formula is MoS_2I_x and iodine induces one hole per formula unit. Although iodine can easily be desorbed from the

DOI: 10.1021/jp512013n
J. Phys. Chem. C 2015, 119, 3918−3922

surface by extensive washing, the removal of substituted or intercalated I_2 is more demanding. Probably, high temperature annealing in vacuum or in H_2S vapors would reduce its doping effect.

Contrary to the positive sign of Seebeck coefficient of MoS_2 grown with I_2, single crystals grown with $TeCl_4$ and Br_2 transport agents show values of $S(300\ K) = -460\ \mu V/K$ and $S(300\ K) = -293\ \mu V/K$, respectively. Other authors previously reported that CVT growth employing $TeCl_4$ and Br_2 transport agents cause n-doping also in WSe_2 and $MoSe_2$ crystals.[12] However, WSe_2 and $MoSe_2$ samples grown with I_2 transport agent display p- and n-doping at room temperature, respectively.[12] Positive Seebeck coefficients were also observed in naturally grown MoS_2 crystal.[28] However, none of these samples displayed a change in S at low temperatures. The smooth transition from holes dominated transport to electrons dominated transport in our MoS_2 sample grown by I_2 indicate that both p and n type of charge carriers are present in the material. We showed before that iodine intercalation could give extra holes. Sulfur vacancies could be instead the cause of extra electrons, as it was observed in WS_2.[13]

In conclusion, we have shown that MoS_2 single crystals grown by the chemical vapor transport method suffer from an unintentional doping by the transport agent molecules. Temperature-dependent electrical and thermal transport measurements clearly reveal the presence of defect and inclusions inside the material, as confirmed by our IBAA and TXRF studies. This shortcoming of CVT grown MoS_2 should be always taken into account in the discussion of its physical properties, especially when exfoliated MoS_2 single layers are foreseen for applications.

EXPERIMENTAL METHODS

First, MoS_2 powder was synthesized by heating a mixture containing stoichiometric amounts of molybdenum (99.9% pure, Alfa Aesar) and sulfur (99.999% pure, Alfa Aesar) at 1000 °C for 7 days in an evacuated and sealed quartz ampule. The mixture was slowly heated from room temperature to 1000 °C for 12 h in order to avoid any explosion due to the strong exothermic reaction and the high volatility of sulfur. From this powder, MoS_2 crystals were grown using chemical vapor transport (CVT) with iodine, bromine, and tellurium tetrachloride as transport agent at ca. 5 mg/cm^3. All quartz tubes used for vapor transport typically have an inner diameter of 16 mm and a length of 20 cm. The total powder charge is 5 g. A very slight excess of sulfur is always included (typically 0.5 wt % of the charge) to ensure the stoichiometry in the resulting crystals. The excess of sulfur is not incorporated into the dichalcogenide crystals but condenses as elemental sulfur onto the wall of the quartz tube at the end of the CVT process. The source and growth zones were kept at 1060 and 1010 °C, respectively, for 7 days in evacuated and sealed quartz ampules. After this time the furnace is turned off, a small fraction of the charge is transported toward the colder end of the tube, forming crystals with diameters of about 2−8 mm and thick tens of microns, with exception of $TeCl_4$, where even 400 μm thicknesses where observed. The resulting crystals were washed with acetone and dried in vacuum. X-ray diffraction study has shown that MoS_2 obtained in this way belongs to the 2H polymorphism (see Supporting Information).

Resistivity measurements in the *ab*-plane and along the *c*-axis were performed in a conventional four-probe configuration after evaporation of chromium/gold contacts. Sketches are shown as insets in Figures 1 and 2. For the ρ_c configuration the outer large circle is the current lead and the point-like contact in the middle is the voltage electrode. For the thermoelectric power measurement the sample was anchored to a ceramic bar on which a temperature gradient (ΔT) was generated by a small heater at one end. The ΔT across the sample was measured by a differential chromel−constantan thermocouple attached to the sample (the details are described elsewhere[29]). Thermal conductivity (κ) was measured by the steady state method, using a reference sample to measure the heat current through the MoS_2 single crystal as described elsewhere.[30]

ASSOCIATED CONTENT

Supporting Information

Experimental details (SEM, XRD, TXRF, IBAA measurements). This material is available free of charge via the Internet at http://pubs.acs.org.

AUTHOR INFORMATION

Corresponding Author

*E-mail andrea.pisoni@epfl.ch (A.P.).

Author Contributions

A.P. and J.J. contributed equally to this work.

Notes

The authors declare no competing financial interest.

ACKNOWLEDGMENTS

The research was supported by the Swiss National Science Foundation. The technical assistance of Dr. R. Gaál is gratefully acknowledged. We thank Stefano Pisoni for help in performing resistivity measurements. We thank N. M. Norbert and M. Cantoni for help in the crystals' characterization. This research project has been supported by the European Commission under the seventh Framework Programme through the "Research Infrastructures" action of the Capacities Programme, NMI3-II, Grant Agreement number 283883.

REFERENCES

(1) Friend, R. H.; Yoffe, A. D. Electronic-Properties of Intercalation Complexes of the Transition-Metal Dichalcogenides. *Adv. Phys.* **1987**, *36*, 1−94.

(2) Friend, R. H.; Beal, A. R.; Yoffe, A. D. Electrical and Magnetic-Properties of Some 1st Row Transition-Metal Intercalates of Niobium Disulfide. *Philos. Mag.* **1977**, *35*, 1269−1287.

(3) Sipos, B.; Kusmartseva, A. F.; Akrap, A.; Berger, H.; Forro, L.; Tutis, E. From Mott State to Superconductivity in 1T-TaS_2. *Nat. Mater.* **2008**, *7*, 960−965.

(4) Wilson, J. A.; Disalvo, F. J.; Mahajan, S. Charge-Density Waves and Superlattices in Metallic Layered Transition-Metal Dichalcogenides. *Adv. Phys.* **1975**, *24*, 117−201.

(5) *G.H.O.I. Chemistry and Organometallic*; Springer-Verlag: Berlin, 1995.

(6) Mak, K. F.; Lee, C.; Hone, J.; Shan, J.; Heinz, T. F. Atomically Thin MoS_2: A New Direct-Gap Semiconductor. *Phys. Rev. Lett.* **2010**, *105*, 1−4.

(7) Novoselov, K. S.; Jiang, D.; Schedin, F.; Booth, T. J.; Khotkevich, V. V.; Morozov, S. V.; Geim, A. K. Two-Dimensional Atomic Crystals. *Proc. Natl. Acad. Sci. U. S. A.* **2005**, *102*, 10451−10453.

(8) Radisavljevic, B.; Radenovic, A.; Brivio, J.; Giacometti, V.; Kis, A. Single-Layer MoS_2 Transistors. *Nat. Nanotechnol.* **2011**, *6*, 147−150.

(9) Yang, L.; Majumdar, K.; Liu, H.; Du, Y.; Wu, H.; Hatzistergos, M.; Hung, P. Y.; Tieckelmann, R.; Tsai, W.; Hobbs, C.; Peide, D. Y. Chloride Molecular Doping Technique on 2D Materials: WS_2 and MoS_2. *Nano Lett.* **2014**, *14*, 6275−6280.

DOI: 10.1021/jp512013n
J. Phys. Chem. C 2015, 119, 3918−3922

(10) Lin, M. W.; Liu, L. Z.; Lan, Q.; Tan, X. B.; Dhindsa, K. S.; Zeng, P.; Naik, V. M.; Cheng, M. M. C.; Zhou, Z. X. Mobility Enhancement and Highly Efficient Gating of Monolayer MoS_2 Transistors with Polymer Electrolyte. *J. Phys. D: Appl. Phys.* **2012**, *45*, 1−6.
(11) Zhang, Y. J.; Ye, J. T.; Matsuhashi, Y.; Iwasa, Y. Ambipolar MoS_2 Thin Flake Transistors. *Nano Lett.* **2012**, *12*, 1136−1140.
(12) Legma, J. B.; Vacquier, G.; Casalot, A. Chemical Vapour Transport of Molybdenum and Tungsten Diselenides by Various Transport Agents. *J. Cryst. Growth* **1993**, *130*, 253−258.
(13) Baglio, J.; Kamieniecki, E.; Decola, N.; Struck, C.; Marzik, J.; Dwight, K.; Wold, A. Growth and Characterization of n-WS_2 and Niobium-Doped p-WS_2 Single Crystals. *J. Solid State Chem.* **1983**, *49*, 166−179.
(14) Zuppiroli, L.; Forro, L. Hopping Conductivity in Polaronic Situations. *Phys. Lett. A* **1989**, *141*, 181−185.
(15) MacDonald, D. K. C. *Thermoelectricity: An Introduction to the Principles*; Dover Publications: Mineola, NY, 2006.
(16) Emin, D. Enhanced Seebeck Coefficient from Carrier-Induced Vibrational Softening. *Phys. Rev. B* **1999**, *59*, 6205−6210.
(17) Aselage, T. L.; Emin, D.; McCready, S. S.; Duncan, R. V. Large Enhancement of Boron Carbides' Seebeck Coefficients Through Vibrational Softening. *Phys. Rev. Lett.* **1998**, *81*, 2316−2319.
(18) Jacimovic, J.; Vaju, C.; Magrez, A.; Berger, H.; Forro, L.; Gaal, R.; Cerovski, V.; Zikic, R. Pressure Dependence of the Large-polaron Transport in Anatase TiO_2 Single Crystals. *Europhys. Lett.* **2012**, *99*, 57005.
(19) Kelly, B. T. *Physics of Graphite*; Applied Science Publishers: Amsterdam, 1981.
(20) Jo, I.; Pettes, M. T.; Ou, E.; Wu, W.; Shi, L. Basal-Plane Thermal Conductivity of Few-Layer Molybdenum Disulfide. *Appl. Phys. Lett.* **2014**, *104*, 1−4.
(21) Yan, R.; Simpson, J. R.; Bertolazzi, S.; Brivio, J.; Watson, M.; Wu, X.; Kis, A.; Luo, T.; Hight Walker, A. R.; Xing, H. G. Thermal Conductivity of Monolayer Molybdenum Disulfide Obtained from Temperature-Dependent Raman Spectroscopy. *ACS Nano* **2014**, *8*, 986−993.
(22) Sahoo, S.; Gaur, A. P.; Ahmadi, M.; Guinel, M. J.-F.; Katiyar, R. S. Temperature-Dependent Raman Studies and Thermal Conductivity of Few-Layer MoS_2. *J. Phys. Chem. C* **2013**, *117*, 9042−9047.
(23) Callaway, J. Model for Lattice Thermal Conductivity at Low Temperatures. *Phys. Rev.* **1959**, *113*, 1046−1051.
(24) Das, S.; Prakash, A.; Salazar, R.; Appenzeller, J. Toward Low-Power Electronics: Tunneling Phenomena in Transition Metal Dichalcogenides. *ACS Nano* **2014**, *8*, 1681−1689.
(25) Thurber, W. R.; Mante, A. J. H. Thermal Conductivity and Thermoelectric Power of Rutile (TiO_2). *Phys. Rev.* **1965**, *139*, 1655−1665.
(26) Benavente, E.; Santa Ana, M. A.; Mendizabal, F.; Gonzalez, G. Intercalation Chemistry of Molybdenum Disulfide. *Coord. Chem. Rev.* **2002**, *224*, 87−109.
(27) Hildebrand, B.; Didiot, C.; Novello, A. M.; Monney, G.; Scarfato, A.; Ubaldini, A.; Berger, H.; Bowler, D. R.; Renner, C.; Aebi, P. Doping Nature of Native Defects in 1T-$TiSe_2$. *Phys. Rev. Lett.* **2014**, *112*, 1−5.
(28) Thakurta, S. G.; Dutta, A. Electrical Conductivity, Thermoelectric Power and Hall Effect in p-Type Molybdenite (MoS_2) Crystal. *J. Phys. Chem. Solids* **1983**, *44*, 407−416.
(29) Jacimovic, J.; Gaal, R.; Magrez, A.; Piatek, J.; Forro, L.; Nakao, S.; Hirose, Y.; Hasegawa, T. Low Temperature Resistivity, Thermoelectricity, and Power Factor of Nb Doped Anatase TiO_2. *Appl. Phys. Lett.* **2013**, *102*, 1−3.
(30) Pisoni, A.; Jacimovic, J.; Barisic, O. S.; Spina, M.; Gaál, R.; Forro, L. Ultra-Low Thermal Conductivity in Organic−Inorganic Hybrid Perovskite $CH_3NH_3PbI_3$. *J. Phys. Chem. Lett.* **2014**, *5*, 2488−2492.

DOI: 10.1021/jp512013n
J. Phys. Chem. C 2015, 119, 3918−3922